A bioorthogonal chemistry approach to the study of biomolecules in their ultrastructural cellular context

Elsland, D.M. van

4

Correlative Light and Electron Microscopy reveals Discrepancy between Gold and Fluorescence Labelling*

Introduction

Fluorescence Microscopy (FM) is a powerful imaging tool that can be employed to track, localise and monitor biomolecules within cellular systems. However, with fluorescence measurements only the position of the labelled biomolecules can be studied in relation to other fluorescently-labelled biomolecules, but the morphology of subcellular structures wherein they reside remains invisible. Conversely, Electron Microscopy (EM) enables observations at nanometer-scale resolution and is therefore often employed to gain ultrastructural characterisation of the subcellular environment pertinent to the biomolecules initially investigated with FM.[1-5]

The location of biomolecules within EM imaged specimen can be visualised upon gold labelling. Colloidal gold is electron dense and, due to its punctate and precise

* Published as part of: Daphne M. van Elsland, Erik Bos, Joanna B. Pawlak, Herman S. Overkleeft, Abraham J. Koster and Sander I. van Kasteren. *J. Microsc.,* **267**, 307-317 (2017). Prof. Gareth Griffiths, Dr. Urška Repnik, and Dr. I. Berlin are kindly acknowledged for critical reading of the manuscript.

labelling pattern, it is favourable for the localisation of biomolecules within structures studied at nanometer scale.[6, 7] Gold labelling can be broadly applied, e.g. in combination with immunocytochemistry (through direct antibody coupling or in combination with protein A), but also with lectins and other binding proteins.[6, 8] This allows recognition of fluorescent reporter proteins (such as green fluorescent protein (GFP)), fluorophores, or direct epitopes studied with FM.[9] The preferred method for preparing biological material for gold labelling is the Tokuyasu cyosectioning technique. This technique is the only post-embedding on-section immunolabelling approach that does not require dehydration by polar solvents before application of affinity markers. It is therefore that thawed crysosections tend to give the highest accessibility of antibodies to the antigens and are the best for most purposes on-section labelling strategies.[10-12]

Besides colloidal gold markers, directly visible in the electron microscope, one can also use Correlative Light and Electron Microscopy (CLEM) to directly visualise fluorescent markers on EM imaged specimen. With CLEM, specific biomolecules and cellular structures can be identified at low magnification with FM, followed by ultrastructural assessment of subcellular location and context with EM.[13, 14] CLEM enables the detection of rare cellular events and allows interpretation of fluorescent labelling on low magnification/large overview images in contrast to colloidal gold markers, which are too small to detect at low magnification. A downside of fluorescence-based CLEM is that correlation of images requires enlargement of the FM image to cover the high magnification EM image. This enlargement results in diffuse fluorescent signals with a diameter of a few hundred nanometers that cannot be related to the exact location of proteins of interest, which can be around 4 nm in diameter and may be associated with organelles as small as 30 nm.[15]

It was envisaged that the center of the fluorescent signals could be found by combining gold labelling and fluorescence-based CLEM in a single experiment. Surprisingly, this combination showed for the lysosomal membrane protein LAMP-1 a discrepancy between the distribution of gold and fluorescent label. To understand the scope and implications of this phenomenon, a series of experiments were devised involving bioorthogonal labelling of cryosections.[16] Bioorthogonal labelling is a chemical labelling strategy whereby firstly a small, physiologically inert chemical group is incorporated into a biomolecule of interest,

which is subsequently reacted with a detection group using a highly selective chemical reaction. With this approach a wide range of biomolecules can be labelled, with high specificity and minimal perturbations.[17, 18] Through the use of bioorthogonal labelling it was possible to compare fluorescence and immunogold labelling of model membrane-associated or soluble epitopes using the same labelling procedures. It was discovered that in particular membrane-associated antigens are strongly labelled with gold particles, whereas the signal of fluorescence labelling of the same target molecules is weak or not detectable.

Results

Defining the problem

In order to determine the position of fluorophore-tagged antigens within cellular ultrastructures, a previously described CLEM strategy was applied for detection and localisation of fluorescent tags[16] and labelled fluorophore-antigen complexes with immuno gold particles. This strategy involves cryosectioning according to the Tokuyasu technique and thus allows fluorescence-based CLEM and immunogold labelling on the same specimen sections. Labelling strategies employed in this study are schematically displayed in all figures and the corresponding symbol legends are shown in Table 1. The fluorescence-gold labelling strategies employed in this study all rely on indirect fluorophore to gold conjugation upon use of antibodies. This indirect fluorophore to gold conjugation has been shown to minimise the possible quenching of the fluorescence signals and is therefore the method of choice to combine fluorescence-based CLEM and immunogold labelling.[19]

Table 1. Symbols legends labelling strategies.

component	symbol
Protein A conjugated gold	
Protein A conjugated AlexaFluor	
IgG antibody	
AlexaFluor conjugated IgG antibody	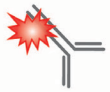
Antigen	
Azide modified antigen	
AlexaFluor alkyne	

It was chosen to apply this strategy to the lysosomal membrane glycoprotein LAMP-1, a major protein component of the lysosomal membrane.[20] LAMP-1 is widely used as a marker for the identification of late endosomes and lysosomes with FM and EM.[21, 22] Bone Marrow derived Dendritic Cells (BM-DCs) were cultured, processed for cryosectioning[23] and sectioned into 75 nm thick sections, followed by primary labelling with a fluorescent (AlexaFluor 647) rat anti mouse LAMP-1 antibody and secondary labelling with 15 nm protein A-coated gold particles after a rabbit anti-rat IgG binding step (Figure 1A, *Strategy*). Sections were then imaged with a confocal microscope, after which sections were stained with uranylacetate and imaged using an electron microscope. The FM and EM images were superimposed (Figure 1A, *CLEM*), and the corresponding label distributions were analysed (Figure 1A, *Label distribution*). To facilitate interpretation of the gold labelling in relation to the fluorescent signals, all gold particles are highlighted with green dots. Upon the morphological appearance of

a visible membrane profile several organelles are depicted white when fluorescent label is associated and yellow when gold label is associated. It was found that the distribution of LAMP-1 gold only partially overlapped with the distribution of LAMP-1 fluorescence, while LAMP-1 fluorescence was always associated with gold label (Figure 1A, *Label distribution*). Note that gold can be localised on fluorescent labels, but not on organelle structures. Moreover, areas with high fluorescence were not highly gold-labelled. Quantification of overlap revealed that only 66% of the gold particles colocalised with fluorescence.

The above results were deemed remarkable, considering that the gold label was directed towards the fluorescent LAMP-1 antibody. To explore whether such label discrepancy represents a general phenomenon associated with combining fluorescence and gold techniques, the CLEM and immunogold approach was tested for non membrane-bound molecules, namely cathepsins papain-like cysteine proteases known to reside within lysosomes. In order to label cathepsins with fluorescence and immunogold, BM-DCs were incubated with a DCG-04 probe, which binds to active cathepsins and contains a bioorthogonal azide-group.[24, 25] After cryo sectioning of BM-DCs, the DCG-04-azide was labelled with an AlexaFluor 488 fluorophore using an on-section copper-catalysed Huisgen cycloaddition (ccHc) reaction.[16] This was followed by an immunogold labelling step directed against the AlexaFluor 488 (Figure 1B, *Strategy*). The distribution of cathepsin gold label corresponded well with the distribution of the cathepsin fluorescence label (Figure 1B, *Label distribution*). Quantification showed that 87% of the gold particles co-localised with the fluorescence signal. These results suggest that the degree of correspondence between gold and fluorescence label distribution may vary with the location of the antigen (i.e. membrane-associated versus soluble).

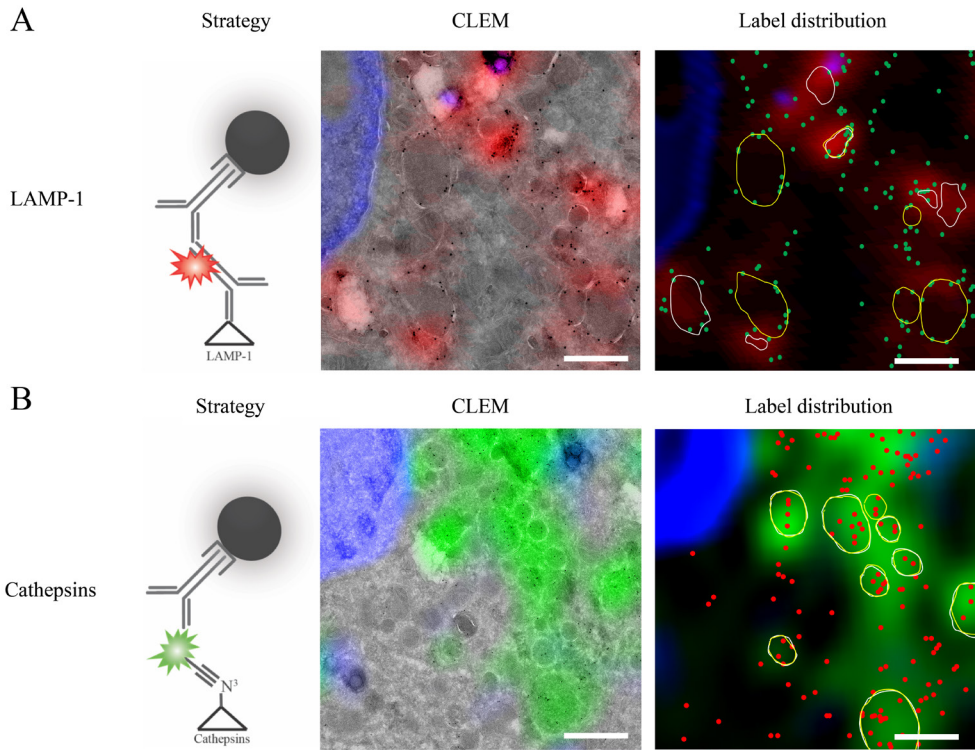

Figure 1. Labelling of LAMP-1 with gold results in different label patterns compared to the labelling of LAMP-1 with fluorescence. (A) BM-DC sections were labelled with a fluorescent AlexaFluor647 (red) rat anti-mouse LAMP-1 antibody, and with protein A-coated gold particles. Gold particle labelling was performed using a rabbit anti-rat binding step (*Strategy*). Representative CLEM image (*CLEM*). Upon the morphological appearance of a visible membrane profile several organelles are depicted white when fluorescent label is associated and yellow when gold label is associated (*Label distribution*). (B) BM-DCs were incubated with DCG-04-azide and were labelled with AlexaFluor488 alkyne (green) and with protein A coated gold directed against AlexaFluor488 using a rabbit anti-AlexaFluor448 binding step (*Strategy*). Representative CLEM image (*CLEM*). Upon the morphological appearance of a visible membrane profile, several organelles are depicted white when fluorescent label is associated, and yellow when gold label is associated (*Label distribution*). Scale bars 500 nm.

Analyzing the problem

In contrast to LAMP-1, the distribution of gold label corresponded well with the distribution of the fluorophore label for cathepsins. Since LAMP-1 and cathepsins are associated with the same organelles, it was anticipated to see predominantly overlap of the LAMP-1 and cathepsin label distributions.[26] To test this, LAMP-1-associated organelles were defined as being positive for cathepsin label and distributions of LAMP-1 gold (Figure 2A, *Strategy*) and LAMP-1 fluorescence

(Figure 2B, *Strategy*) in relation to these cathepsin-positive organelles were analysed. As expected, association of LAMP-1 with cathepsin-positive organelles was confirmed with immunogold labelling (Figure 2A, *CLEM and Label distribution*). However, immunofluorescence labelling of LAMP-1 showed that LAMP-1 also associated with cathepsin-negative organelles and that cathepsin positive vesicles are not always associated with LAMP-1 (Figure 2B). To exclude the possibility that the secondary antibody in the gold label strategy represented in Figure 2A would influence the labelling, the protein A gold was substituted for protein A AlexaFluor 647 (Figure 2C, *Strategy*) and the result of this strategy (Figure 2C, *label distribution*) was compared with the results shown in Figure 2B. Statistical colocalisation analysis (Figure 2C, *colocalisation*) showed that substitution of protein A gold by protein A AlexaFluor 647 resulted in a label distribution similar to the distribution shown in Figure 2B. Collectively, these results indicate that the application of gold particles within a label strategy influences the immunodetection of antigens on sections.

Testing the hypothesis

The results presented so far show that the distribution of immunogold label for LAMP-1 does not completely correlate with immunofluorescent labelling of the same antigen. As this was prominently observed for the LAMP-1 epitope, but not for the cathepsin epitope, it was postulated that there could be an effect of the immediate surrounding of the epitope on the ability of the gold conjugates to bind to cognate epitopes. Since LAMP-1 is a membrane-bound molecule while cathepsin is soluble, it was hypothesised that immunogold labels membrane-bound molecules differently from soluble epitopes. It was thus set out to install the same bioorthogonal group used to label cathepsins via the DCG-04 probe on a membrane-associated epitope, creating the same covalent fluorophore introduction in a membrane associated context. This was achieved by installing the bioorthogonal group on sialylated glycans,[27] as these constitute parts of membrane-bound molecules.

Jurkat cells were incubated with Ac_4-N-azidoacetylmannosamine (Ac_4-ManNAz), to add a bioorthogonal functionality to sialylated glycans under conditions reported previously.[16] Cryo sections from these cells were subjected to the same labelling strategy as used for the cathepsins above. To eliminate the possibility that a different cell type and/or rearrangement of the bioortogonal group would

influence either the binding of AlexaFluor 488 alkyne or recognition of AlexaFluor 488 by anti AlexaFluor 488 IgG, modified epitopes were first doublelabelled with AlexaFluor alkyne and protein A AlexaFluor (Figure 3A and B, S*trategy*). Similar overlap of the two fluorophores was observed for both epitopes (Figure 3A and B, *Label distribution*) with no significant difference between the two azide-modified epitopes (Figure 3B, *Colocalisation*), meaning that the affinities of the two labels were not altered upon the epitope or cell type change. Next, the sialylated glycans were doublelabelled and protein A AlexaFluor was substituted for protein A gold (Figure 3C, *Strategy*). It was found that the gold label localised primarily on the plasma membrane, whereas the fluorescent signal predominantly labelled intracellular structures (Figure 3C, *CLEM*). Quantification of colocalisation (Figure 3C, *Label distribution*) revealed that again only 64% of the gold label co-localised with the fluorescent foci, lending credence to the hypothesis that the cellular location of an epitope influences the degree of gold labelling. For soluble epitopes the degree of gold label is relatively low compared to the fluorescent signal, whereas the membrane-bound epitopes get highly labelled with gold, even when the fluorescence label is poorly or not detectable at all with confocal microscopy.

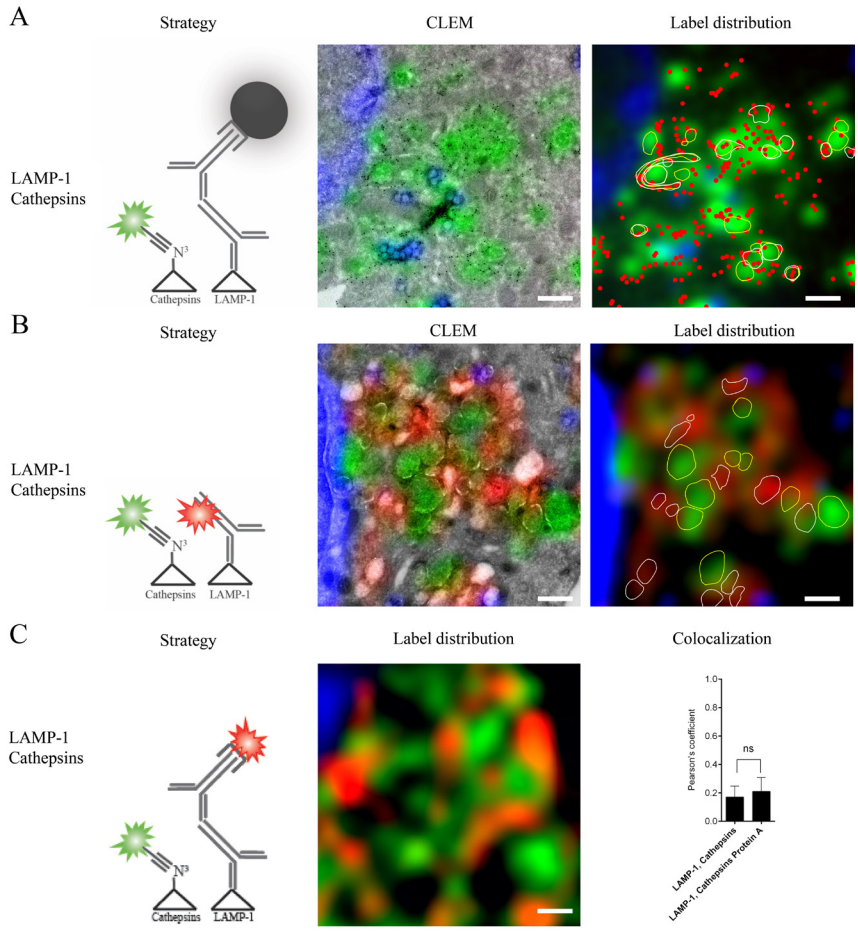

Figure 2. Labelling with gold particles shows a different antigen distribution than with fluorescent labelling. (A) BM-DCs were incubated with DCG-04-azide and labelled with AlexaFluor488 alkyne (green). Sections were subsequently labelled with anti-LAMP-1 and protein A-coated gold directed against the LAMP-1 antibody using a rabbit anti-rat binding step (S*trategy*). CLEM images obtained (*CLEM*) were analysed for label distribution and gold distribution is marked with red dots. Structures that are positive for LAMP-1 gold are depicted in white and structures positive for cathepsin fluorescence are depicted in yellow. (B) BM-DCs were incubated with DCG-04-azide and were labelled on section with AlexaFluor488 alkyne (green). Sections were subsequently labelled with fluorescent AlexaFluor647 anti-LAMP-1 (red) (*Strategy*). CLEM images obtained (*CLEM*) were analysed for label distribution. Structures positive for LAMP-1 fluorescence are depicted in white and structures positive for cathepsin fluorescence in yellow. (C) BM-DCs were incubated with DCG-04-azide and were labelled on section with TAMRA alkyne (green). Sections were subsequently labelled with anti-LAMP-1 and protein A AlexaFluor488 fluorophore (red) directed against the LAMP-1 antibody using a rabbit anti-rat binding step (*Strategy*). A representative confocal image of this sample is shown in *Fluorescence*. Colocalisation analysis of the labelling sequences in (B) and (C) (*Colocalisation*). Scale bars, 500 nm.

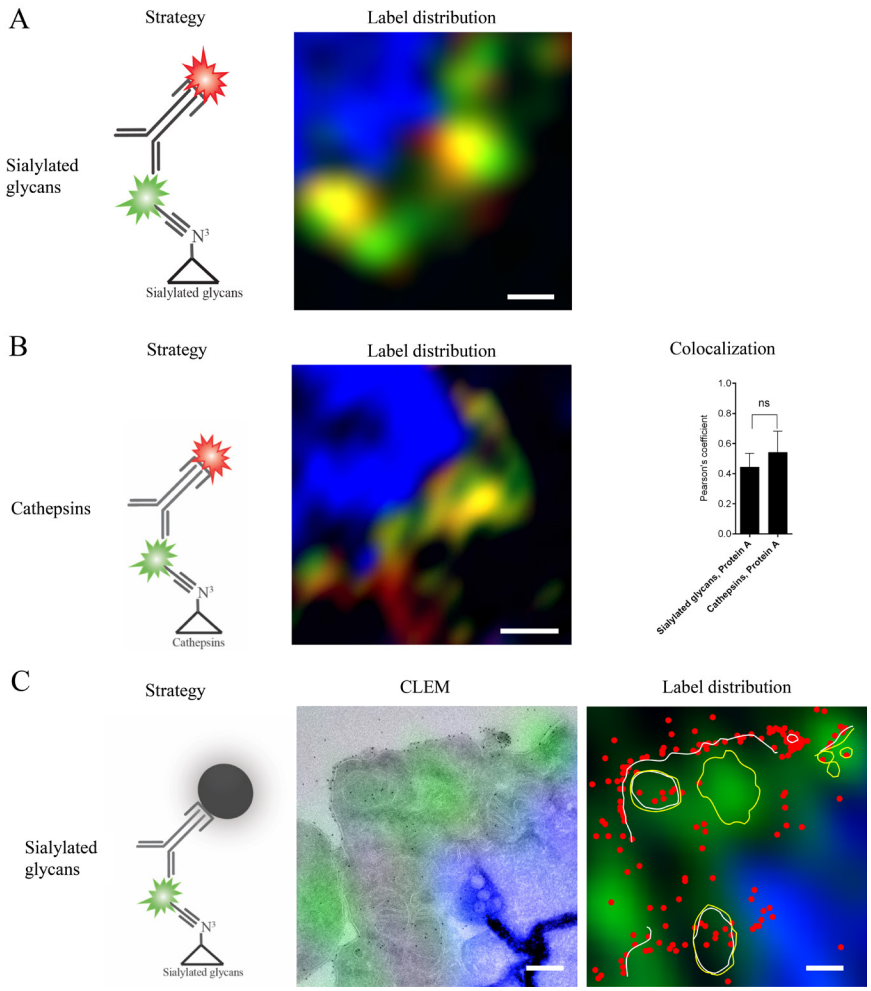

Figure 3. The cellular location of an epitope influences gold labelling, resulting in a discrepancy between fluorescence and gold label distribution. (A) Jurkat cells were incubated with N-azidoacetylmannosamine and were labelled on section with AlexaFluor488 alkyne (green). Sections were subsequently labelled with a AlexaFluor647 protein A fluorophore directed against the AlexaFluor488 using a rabbit anti-rat binding step (*Strategy*). (B) BM-DCs incubated with DCG-04-azide were labelled on section with AlexaFluor488 alkyne (green) and protein A AlexaFluor647 (red) directed toward AlexaFluor488 using a rabbit anti-AlexaFluor488 binding step. Colocalisation analysis of sialylated glycans and protein A compared to cathepsins and protein A (*Colocalisation*). (C) Jurkat cells were incubated with N-azidoacetylmannosamine and were labelled on section with AlexaFluor488 alkyne (green). Gold particle labelling was performed using a rabbit anti-AlexaFluor448 binding step (*Strategy*). Representative CLEM image (CLEM). Organelles positive for sialylated glycan-fluorescence are depicted in yellow and organelles positive for sialylated glycan-gold are depicted in white. The distribution of these spheres is displayed in the context of the label distribution (*Label distribution*). Scale bar 500 nm.

Conclusion

In order to translate information of FM studies to EM analysis, biomolecules initially observed with the former need to be labelled in a manner compatible with EM. Traditionally this is performed using immunogold labelling of fluorescently detected biomolecules. Here the discrepancies arising between distributions of fluorescence and gold labelling were identified and explored. It was found that a subset of cathepsin-positive organelles is negative for LAMP-1 when labelling is done by fluorescence, but positive for LAMP-1 when labelling is done with gold particles. Variations in label distributions can be explained by marker heterogeneity in phagosomal, endosomal and lysosomal structures.[28-30] However, such heterogeneity cannot explain that the label distribution pattern changes upon changing the type of label (gold vs fluorescent label). It was reasoned that the antigen detection level could change upon changing the type of label, but that the label distribution pattern should not.

In a comparison of fluorescent and gold label it can be argued that the localisation of diffuse enlarged fluorescent signals may result in a less distinct mapping of positive structures, and that fluorescence can be difficult to detect when label density is weak, which is especially the case for fluorescence labelling on non-dense structures such as membranes. However, since the fluorescence intensity is related to the concentration of the epitope, there should still be an overlap of fluorescence and gold label,[31] and this is not expressed by the observed discrepancy.

On top of this gold labelling may show different antigen detection levels. Variations in labelling of conjugated gold particles have been previously reported by Griffiths and Hoppeler, describing variations in immunogold labelling efficiencies for the ER, Golgi apparatus and viral membranes.[32] In their study the ER membranes were found to exhibit the highest labelling efficiency compared to the Golgi apparatus or viral membranes. These observations are supported by others noting profound variations in immunogold labelling efficiency between different cellular compartments and structures.[33-35] It is generally considered that cross-linking of target molecules by fixatives, as well as steric hindrance and valency of both target and ligand molecules constitute factors that influence labelling efficiency.[36] Other investigators report that the density of cellular material affects the labelling efficiency as well. In dense secretory granules, there

is almost only surface labelling whereas the less dense endoplasmic reticulum gets more prominently labelled.[37] It was postulated that these epitope availability effects more strongly affect gold labelling compared to fluorescence labelling, resulting in the discrepancies observed between these labelling strategies.

If epitopes of interest are found in various structures within the same specimen, gold labelling may result in a biased detection of target molecules. As a consequence it may be argued that in this context fluorescence labelling is preferable to gold labelling. However, to reach the punctuality of the gold particles, the detection of these fluorescence labels needs to be at a higher resolution. Super-resolution microscopy techniques, such as STORM and PALM, may serve this purpose as these techniques allow to precisely localise molecules at a resolution of a few nanometers. Moreover, examples of their applications to CLEM have yet been explored.[15, 38] Another approach resulting in high resolution labelling includes labels capable of polymerizing diaminobenzidine (DAB) . It has been shown that photooxidation-based polymerisation of DAB occurs within a few nanometers away of the epitope.[39-42] Application of these high resolution methods could pave the way to provide alternative labels for accurate mapping in correlative FM and EM studies.

Experimental

Specimen preparation

BM-DCs and Jurkat cells were cultured as described elsewhere[16]. BM-DCs were incubated for 2 hours with DCG-04-azide [43] (final concentration of 10 µM), after which the cells were washed with PBS and kept for 2 h in fresh medium. Jurkat cells were incubated for 3 days with 50 µM of N-azidoacetylmannosamine (MannAz, Invitrogen) from stock solutions in DMSO.

Samples were prepared for cryosectioning as described elsewhere [16, 44]. Briefly, BM-DCs and Jurkat cells were fixed for 24 h in freshly prepared 2% PFA in 0.1 M phosphate buffer. Fixed cells were embedded in 12% gelatin (type A, bloom 300, Sigma) and cut with a razor blade into 0.5 mm^3 cubes. The sample blocks were infiltrated in phosphate buffer containing 2.3 M sucrose for 3 h. Sucrose-infiltrated sample blocks were mounted on aluminum pins and plunged in liquid nitrogen. The frozen samples were stored in liquid nitrogen.

Ultrathin cell sections of 75 nm were obtained essentially as described elsewhere[16]. Briefly, the frozen sample was mounted in a cryo-ultramicrotome (Leica). The sample was trimmed to yield a squared block with a front face of about 300 x 250 µm (Diatome trimming tool). Using a diamond knife (Diatome) and antistatic device (Leica) a ribbon of 75 nm thick sections was produced that was retrieved from the cryochamber with the lift-up hinge method[45]. A droplet of 1.15 M sucrose was used for section retrieval.

Obtained sections were transferred to a specimen grid previously coated with formvar and carbon grids were additionally coated with 100 nm FluoroSpheres carboxylate-modified (350/440) (Life Technologies).

On-section labelling

Sections that were click-labelled with AlexaFluor488/TAMRA alkyne and immunogold-labelled were labelled as follows; thawed cryosections on an EM grid were left for 30 minutes on the surface of 2% gelatin in phosphate buffer at 37°C. Subsequently grids were incubated on drops of PBS/glycine and PBS/glycine containing 1% BSA. Grids were then incubated on top of the ccHc- cocktail (0.1 M HEPES pH 7.3, 1 mM $CuSO_4$, 10 mM sodium ascorbate, 1 mM THPTA ligand, 10

mM amino-guanidine, 5 µM AlexaFluor488/TAMRA alkyne (Invitrogen) for 1 h and washed 6 times with PBS. Sections were then blocked again with PBS/Glycine containing 1% BSA after which the grids were incubated for 1 h with 0.1 M PBS/glycine 1% BSA (blocking solution) supplemented with a rabbit IgG anti Alexa 488 antibody (Invitrogen). After washing with PBS/Glycine and blocking with PBS/glycine 0.1% BSA, grids were incubated for 20 minutes on PBS/glycine 1% BSA supplemented with protein A coated 10 or 15 nm goldparticles (CMC, Utrecht University). Grids were then washed with PBS, labelled with DAPI and additionally washed with PBS and aquadest. In case of protein A AlexaFluor labelling, protein A-coated goldparticles were replaced with protein A Alexa 488 or protein A Alexa 647 (20 µg/ml).

In case of immunofluorescence and immunogold labelling against LAMP-1 thawed cryosections on an EM grid were left for 30 minutes on the surface of 2% gelatin in phosphate buffer at 37°C. Grids were washed 5 times with PBS/glycine and blocked with PBS/glycine containing 1% BSA after which the grids were incubated for 1 h with PBS/glycine 1% BSA supplemented with a rat anti-mouse LAMP-1 AlexaFluor647 (Biolegend, Cat. 121609). Grids were then washed 5 times with PBS/glycine and blocked again with PBS/glycine containing 1% BSA after which the grids were incubated for 1 h with PBS/glycine 1% BSA supplemented with a rabbit IgG anti-rat (Nordic Immunology). After washing with PBS/glycine and blocking with PBS/glycine 0.1% BSA, grids were incubated for 20 minutes with PBS/glycine 1% BSA supplemented with protein A coated 10/15 nm goldparticles (CMC, Utrecht University). Grids were then washed with PBS, labelled with DAPI and additionally washed with PBS and aquadest. In case of protein A Alexa labelling, protein A-coated 10/15 nm goldparticles were replaced for protein A Alexa 488 or protein A Alexa 647 (20 µg/ml).

In case click labelling and LAMP-1 labelling were performed on the same section, click labelling was preformed prior to the LAMP-1 labelling steps.

Microscopy and correlation

The CLEM approach used was adapted from Vicidomini et al. and has been described elsewhere[16]. Briefly, grids containing the sample sections were washed with 50% glycerol and placed on glass slides (precleaned with 100% ethanol). Grids were then covered with a small drop of 50% glycerol, after which a coverslip

was mounted over the grid. Coverslips were fixed using Scotch Pressure-Sensitive Tape. Samples were imaged with a Leica TCS SP8 confocal microscope (63x oil lens, N.A.=1.4). After confocal microscopy the EM grid with the sections was removed from the glass slide, rinsed in distilled water and incubated for 5 minutes on droplets of an aqueous solution containing 2% methylcellulose and 6% uranyl acetate. Excess of methylcellulose/uranyl solution was blotted away and grids were air-dried. EM imaging was performed with a Tecnai 20 transmission electron microscope (FEI) operated at 120 kV acceleration voltage.

Correlation of confocal and EM images was performed in Adobe Photoshop CS6. In Adobe Photoshop, the FM image was copied as a layer into the EM image and made 50% transparent. Transformation of the FM image was necessary to match it to the larger scale of the EM image. This was performed via isotropic scaling and rotation using interpolation settings; bicubic smoother. Alignment at low magnification was carried out with the aid of nuclear DAPI staining in combination with the shape of the fluorescently labelled cells. At high magnification alignment was performed using the fiducial beads [46].

Colocalisation analysis and quantification of label distributions

Upon the morphological appearance of a visible membrane profile organelles were depicted either positive for gold or for fluorescence. For the determination of structures positive for gold only structures positive for two or more particles were depicted.

Colocalisation of gold and fluorescence was calculated as a percentage by quantification of the overlap of gold and fluorescence using the count tool in Photoshop. With this strategy gold particles were counted that either colocalised with fluorescence or did not colocalise with fluorescence.

The Pearson coefficient was determined on magnified confocal images of protein A double labelled samples using the Coloc2 function in ImageJ after background was corrected to eliminate nonspecificity. These images were obtained in Adobe Photoshop CS6 upon CLEM correlation.

References

1. S. A. Predescu, D. N. Predescu, B. K. Timblin, R. V. Stan and A. B. Malik, *Mol Biol Cell*, 2003, **14**, 4997-5010.
2. H. Robenek, O. Hofnagel, I. Buers, M. J. Robenek, D. Troyer and N. J. Severs, *J Cell Sci*, 2006, **119**, 4215-4224.
3. M. Boonen, C. Staudt, F. Gilis, V. Oorschot, J. Klumperman and M. Jadot, *J Cell Sci*, 2016, **129**, 557-568.
4. D. Sarnataro, A. Caputo, P. Casanova, C. Puri, S. Paladino, S. S. Tivodar, V. Campana, C. Tacchetti and C. Zurzolo, *PLoS One*, 2009, **4**, e5829.
5. S. I. Choi, Y. S. Maeng, T. I. Kim, Y. Lee, Y. S. Kim and E. K. Kim, *PLoS One*, 2015, **10**, e0119561.
6. G. Griffiths, in *Fine Structure Immunocytochemistry*, Springer Berlin Heidelberg, 1993, 9-25.
7. T. M. Mayhew and J. M. Lucocq, *Histochem Cell Biol*, 2008, **130**, 299-313.
8. W. P. Faulk and G. M. Taylor, *Immunochemistry*, 1971, **8**, 1081-1083.
9. M. S. Sirerol-Piquer, A. Cebrian-Silla, C. Alfaro-Cervello, U. Gomez-Pinedo, M. Soriano-Navarro and J. M. Verdugo, *Micron*, 2012, **43**, 589-599.
10. K. T. Tokuyasu, *J Cell Biol*, 1973, **57**, 551-565.
11. J. W. Slot and H. J. Geuze, *Nat Protoc*, 2007, **2**, 2480-2491.
12. P. Webster, H. Schwarz and G. Griffiths, *Methods Cell Biol*, 2008, **88**, 45-58.
13. P. de Boer, J. P. Hoogenboom and B. N. Giepmans, *Nat Meth*, 2015, **12**, 503-513.
14. B. N. Giepmans, *Histochem Cell Biol*, 2008, **130**, 211-217.
15. S. Watanabe, A. Punge, G. Hollopeter, K. I. Willig, R. J. Hobson, M. W. Davis, S. W. Hell and E. M. Jorgensen, *Nat Meth*, 2011, **8**, 80-84.
16. D. M. van Elsland, E. Bos, W. de Boer, H. S. Overkleeft, A. J. Koster and S. I. van Kasteren, *Chem Sci*, 2016, **7**, 752-758.
17. M. Grammel and H. C. Hang, *Nat Chem Biol*, 2013, **9**, 475-484.
18. D. M. van Elsland, E. Bos, H. S. Overkleeft, A. J. Koster and S. I. van Kasteren, *J Chem Biol*, 2015, **8**, 153-157.
19. I. K. Kandela and R. M. Albrecht, *Scanning*, 2007, **29**, 152-161.
20. E. L. Eskelinen, *Mol Aspects Med*, 2006, **27**, 495-502.
21. E. van Meel and J. Klumperman, *Histochem Cell Biol*, 2008, **129**, 253-266.
22. H. Appelqvist, P. Wäster, K. Kågedal and K. Öllinger, *J Mol Cell Biol*, 2013, **5**, 214-226.
23. P. J. Peters, in *Curr Protoc Cell Biol*, John Wiley & Sons, Inc., 2001.
24. J. R. Pungercar, D. Caglic, M. Sajid, M. Dolinar, O. Vasiljeva, U. Pozgan, D. Turk, M. Bogyo, V. Turk and B. Turk, *The FEBS journal*, 2009, **276**, 660-668.
25. D. Greenbaum, K. F. Medzihradszky, A. Burlingame and M. Bogyo, *Chem Biol*, 2000, **7**, 569-581.

26. D. Bromme, *Curr Protoc Protein Sci,* **Chapter 21**, Unit 21 22.
27. E. Saxon and C. R. Bertozzi, *Science*, 2000, **287**, 2007-2010.
28. J. Huotari and A. Helenius, *EMBO J*, 2011, **30**, 3481-3500.
29. J. P. Luzio, P. R. Pryor and N. A. Bright, *Nat Rev Mol Cell Biol*, 2007, **8**, 622-632.
30. R. M. Henry, A. D. Hoppe, N. Joshi and J. A. Swanson, *J Cell Biol*, 2004, **164**, 185-194.
31. K. Tohda, H. Lu, Y. Umezawa and M. Gratzl, *Anal Chem*, 2001, **73**, 2070-2077.
32. G. Griffiths and H. Hoppeler, *J Histochem Cytochem*, 1986, **34**, 1389-1398.
33. G. Posthuma, J. W. Slot and H. J. Geuze, *J Histochem Cytochem*, 1984, **32**, 1028-1034.
34. J. Tooze, M. Hollinshead, R. Frank and B. Burke, *J Cell Biol*, 1987, **105**, 155-162.
35. J. Lucocq, *J Anat*, 1994, **184 (Pt 1)**, 1-13.
36. J. G. White, M. D. Krumwiede and G. Escolar, *Am J Pathol*, 1999, **155**, 2127-2134.
37. e. H. Catherine Rabouille, M. A. Nasser *Humana Press*, 1999, 125-144.
38. N. de Souza, *Nat Meth*, 2015, **12**, 37-37.
39. G. M. Gaietta, T. J. Deerinck and M. H. Ellisman, *Cold Spring Harb Protoc*, 2011, **2011**, pdb top94.
40. G. E. Sosinsky, G. M. Gaietta, G. Hand, T. J. Deerinck, A. Han, M. Mackey, S. R. Adams, J. Bouwer, R. Y. Tsien and M. H. Ellisman, *Cell Commun Adhes*, 2003, **10**, 181-186.
41. K. Cortese, A. Diaspro and C. Tacchetti, *J Histochem Cytochem*, 2009, **57**, 1103-1112.
42. J. T. Ngo, S. R. Adams, T. J. Deerinck, D. Boassa, F. Rodriguez-Rivera, S. F. Palida, C. R. Bertozzi, M. H. Ellisman and R. Y. Tsien, *Nat Chemical Biol*, 2016, **12**, 459-465.
43. S. Hoogendoorn, G. H. van Puijvelde, J. Kuiper, G. A. van der Marel and H. S. Overkleeft, *Angew Chem Int Ed Engl*, 2014, **53**, 10975-10978.
44. P. J. Peters, E. Bos and A. Griekspoor, *Curr Protoc Cell Biol*, 2006, **Chapter 4**, Unit 4 7.
45. E. Bos, C. SantAnna, H. Gnaegi, R. F. Pinto, R. B. Ravelli, A. J. Koster, W. de Souza and P. J. Peters, *J Struct Biol*, 2011, **175**, 62-72.
46. J. Kuipers, T. J. Ham, R. D. Kalicharan, A. Veenstra-Algra, K. A. Sjollema, F. Dijk, U. Schnell and B. N. G. Giepmans, *Cell Tissue Research*, 2015, **360**, 61-70.